Proceedings of the 9th International Conference on Civil Structural and Transportation Engineering (ICCSTE 2024)
Chestnut Conference Centre - University of Toronto, Toronto, Canada – June 13-15, 2024
Paper No. 249
DOI: 10.11159/iccste24.249

Orthotropic Plate Analysis Model For Estimating Live Load Moment And Deflections In Reinforced Concrete Bridge Deck Slabs Between Longitudinal Girders

Kousai Razouk[1], Aravindan Ramadoss[2], Khaled Sennah[3], Ahmed Hamed[4]
[1]Toronto Metropolitan University, Toronto, Ontario
krazouk@torontomu.ca
[2]Toronto Metropolitan University Toronto, Ontario
agr12112000@gmail.com
[3]Toronto Metropolitan University Toronto, Ontario
ksennah@torontomu.ca
[4]Toronto Metropolitan University Toronto, Ontario
ahmed.hamed@torontomu.ca

Abstract - The equation for calculating the applied transverse moment in reinforced concrete deck slab in slab-on-girder bridges under truck loading in the Canadian Highway Bridge Design Code is dated back to 1930. It does not include the effect of the transverse-to-longitudinal flexural stiffness and the torsional stiffness. In addition, the code does not provide equations for the longitudinal moment and deflection. This paper presents the application of the orthotropic plate theory to determine the applied transverse and longitudinal moment and deflection under different truck loading conditions. The key parameters considered in this study included the slab span ranging from 1 m to 4 m, single- or two-lane loaded with Canadian trucks, different truck axles, and transverse-to-flexural stiffness ratios ranging from 1 to 4. The data generated from this study was used to develop empirical equations for the transverse and longitudinal moments for ultimate and fatigue limit state design and deflection for serviceability limit state design.

Keywords: Bridge decks, bridge analysis, orthotropic plate theory, truck loading, design method.

1. Introduction

Reinforced concrete decks spanning normal to traffic direction are used in slab-on-girder bridges shown in Fig. 1 [1]. In 1930, Westergaard [2] provided the basis for the design moments in bridge slabs due to concentrated loads. He assumed that the concrete slab acts as a homogeneous elastic slab. The basic equation by Westergaard [2] formed the basis of the Canadian Standard for Design of Highway Bridges, CSA-S6-88, [3] to calculate the transverse moment in case the main reinforcement is perpendicular to traffic. This equation continued to be the basis for design in the Canadian Highway Bridge Design Code of 2019, CSA-S6:19 [1]. The unfactored live moment is obtained from this equation per meter width for a simple span as follows:

$$\text{Moment (kN.m/m)} = \frac{(S_e + 0.6)\,P}{10} \tag{1}$$

Where S_e = slab span between girders (m), and P = 87.5 kN (wheel load of axle 4 in the CL-W truck specified in CSA-S6:19).

The 1996 AASHTO Standard Specifications for Highway Bridges [4] adopted Westergaard's equation for the live load moment for simple spans using imperial units for HS 20 truck loading as follows:

$$\text{Moment (Ib.ft /ft)} = \left(\frac{S_e+2}{32}\right) P_{20} \tag{2}$$

Where P_{20} = the wheel load of 16 kip, and S_e = the slab span (ft).

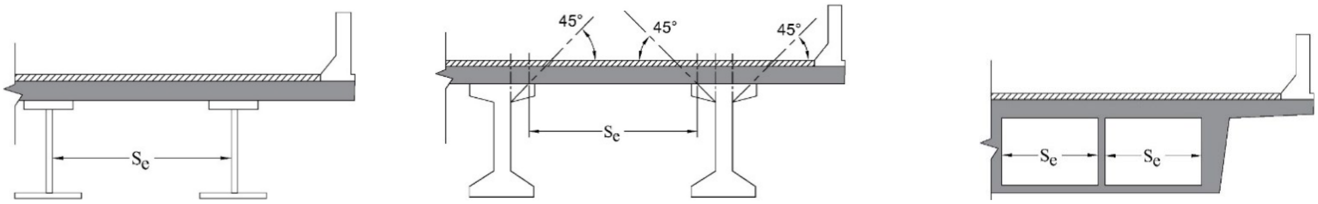

a) Slab on steel girders b) Slab on precast concrete girders c) Slab in a concrete cellular bridge

Fig. 1. Deck slab span between girders (CSA, 2019).

The AASHTO LRFD Bridge Design Specifications of 1998 and 2020 [5, 6] adopted another simplified method for cast-in-place, cast-in-place with stay-in-place concrete formwork, precast and post-tensioned concrete slab deck called Equivalent Strip Method. The designer may analyze the deck slab as a continuous one-way slab supported over girders and subjected to single or twin-truck axles. Then, the resulting moment is modified by dividing it by a distribution width to obtain the live load bending moment per unit width. The widths of the primary strip for the positive and negative moments are specified as ($26.0+6.6S_e$) and ($48.0+3.0S_e$), respectively; Se is the spacing of supporting components in the feet.

CSA-S6:19 specifies that the positive and negative longitudinal moments in the deck slab for distribution of wheel loads shall be taken as $120/(S_e^{0.5})$%, without exceeding 67%, of the maximum transverse moment intensity obtained from equation (1). Again, this provision does not include the effect of the flexural stiffness ratio in calculations.

This paper describes the parametric study, using the orthotropic plate theory, to determine the live load moments and deflection in concrete deck slabs between longitudinal girders when subjected to Canadian truck loading. The key parameters considered in this study included the slab span, single- or two-lane loaded with Canadian trucks, different truck axles, and transverse-to-flexural stiffness ratio. The data generated from this study was used to develop empirical equations for the transverse and longitudinal moments for ultimate and fatigue limit state design and deflection for serviceability limit state design.

2. Orthotropic Plate Theory

In bridge superstructures, due to the complexity of the distribution of forces from the deck slab to the girders, the analysis of the deck-girders system has been an area of research. In 1975, Cusens and Pama [7] presented a structural analysis method for bridge slabs based on the orthotropy plate theory by considering them an equivalent thin plate with different torsional and flexural properties in both orthogonal directions. They provided the solution of the following general differential equations for bending and twisting moments of an orthotropic thin plate [8].

$$D_x \frac{\partial^4 w}{\partial x^4} + 2H \frac{\partial^4 w}{\partial x^2 \partial y^2} + D_y \frac{\partial^4 w}{\partial y^4} = q(x,y) \tag{3}$$

$$H = D_1 + 2D_{xy} \tag{4}$$

$$M_x = -\left(D_x \frac{\partial^2 w}{\partial x^2} + D_1 \frac{\partial^2 w}{\partial y^2}\right) \tag{5}$$

$$M_y = -\left(D_y \frac{\partial^2 w}{\partial y^2} + D_1 \frac{\partial^2 w}{\partial x^2}\right) \tag{6}$$

$$M_{xy} = 2D_{xy} \frac{\partial^2 w}{\partial x \, \partial y} \tag{7}$$

Where: D_x = flexural rigidity in the strong direction; D_y = flexural rigidity in the weak direction; D_1 = torsional rigidity contribution from the strong and the weak direction rigidities; D_{xy} = torsional rigidity; H = sum of the torsional rigidity contribution from the strong and weak direction rigidities (D_1) and torsional rigidity (D_{xy}); w(x,y) = vertical plate deflection in the Cartesian coordinate system; and q(x,y) = applied transverse load in the Cartesian coordinate system.

The analytical solution of equation (3), depends on the value of H relative to D_x and D_y. as shown in equation (8). For reinforced concrete slab, the torsional parameter, α, equals 1 [9] and the solution has equal and real roots:

$$H=\alpha\sqrt{D_x\, D_y} \tag{8}$$

$$\alpha = 1 \tag{9}$$

Bakht et al. [10] developed the PLATO program based on the solution of equation (3) by Cusens and Pama [7] and used the basic equations for finite plates to solve for moments and deflections at any location on the plate. The PLATO program was verified before using data from field tests and can be found elsewhere [11, 12]. In this research on a reinforced concrete slab, Poisson's ratio was taken as 0.2 to assist in obtaining the values of D_1 and D_{xy} based on equations (4), (8), and (9).

3. Parametric Study

A parametric study was conducted on a concrete reinforced deck bridge slab with a thickness of 200 mm to assist in obtaining a reference flexural stiffness in the strong direction of the slab, Dx. Then, using the above equations, D_y, D_{xy}, and D1 values were obtained for different values of flexural stiffness ratio, D, taken as D_x /D_y. The D values considered in this study were 1, 1.25, 1.5, 1.75, 2, 2.5, 3, 3.5, and 4, while the slab span, Se, was taken 1, 1.5, 2, 2.5, 3, 3.5, and 4 m.

Figure 2 shows the elevation, cross-section, and plan view of CL-W truck loading [1]. Two types of trucks were considered in this study: the CL-625 truck, which is used in all Canadian Provinces except Ontario, and the CL-625-ONT truck, which is used in Ontario for bridge design. One may notice that axles 2 and 3 of the CL-625-ONT truck are greater than those for the CL-625 truck by 12%. Figure 3 shows the different truck loading conditions considered in this study. PLATO program can model wheel loads using the footprint dimensions of the tire patches as shown in Fig. 3(a), with v = 250 mm and u = 600 mm in the case of the wheel load of axle 4 in Fig. 2, for example. For a short slab span, one wheel was considered for the single-truck case as depicted in Figs. 3(b) and 3(c) using truck axle 4 and axles 2 and 3, respectively. For a wider slab span, two adjacent wheels for the two adjacent truck cases were considered, as depicted in Figs. 3(d) and 3(e) using truck axle 4 and axles 2 and 3, respectively, with transverse distance between the wheels of 1.2 m. It should be noted that a third load case scenario, not shown in Fig. 3, considered all 5 axles of the truck applied on the deck slab in a similar fashion as those in Figs. 3(c) and 3(e). All these loading cases were considered for ultimate limit state (ULS) and serviceability limit state (SLS2) designs [1]. These loading cases were used to obtain the greatest transverse moment, longitudinal moment and deflection for each S_e and D values mentioned earlier. For fatigue limit state (FLS) design, the Canadian Highway Bridge Design Code [1] specifies a single truck with only axles 2 and 3 to obtain the applied moments, with distance between wheels in direction of slab span of 1.8 m. In this case, the loading case in Fig. 3(c) was used for short spans (S_e = 1 to 3 m), while the loading case in Fig. 3(f) was used for larger spans (S_e = 3.5 and 4 m).

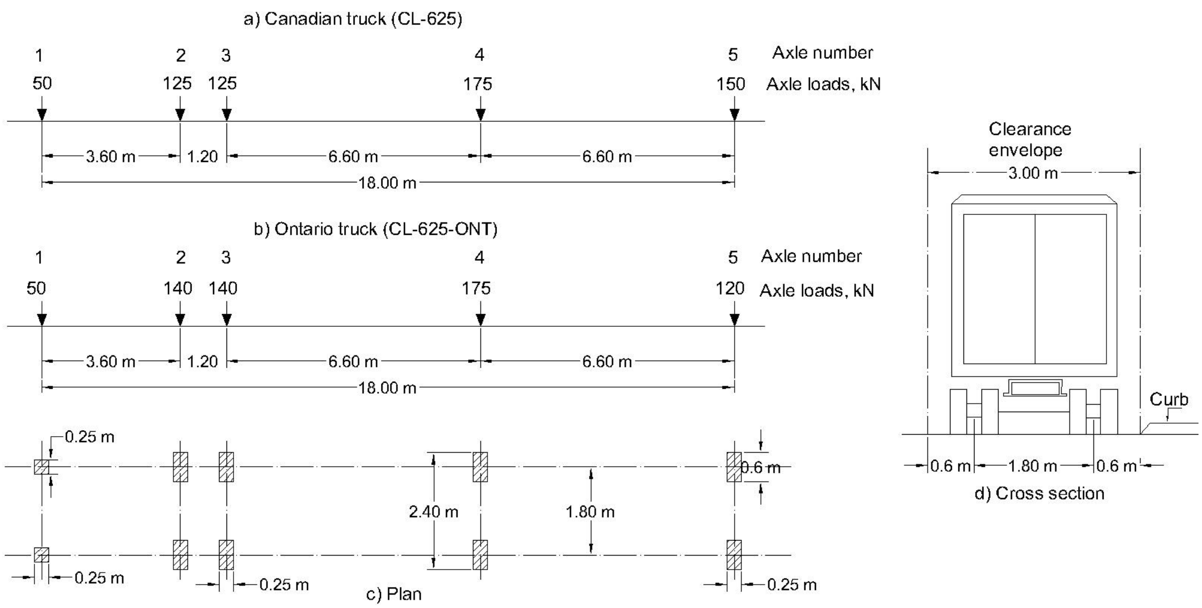

Fig. 2. Elevation, cross-section, and plan view of CHBDC truck loading (CL-625 and CL-625-ONT)

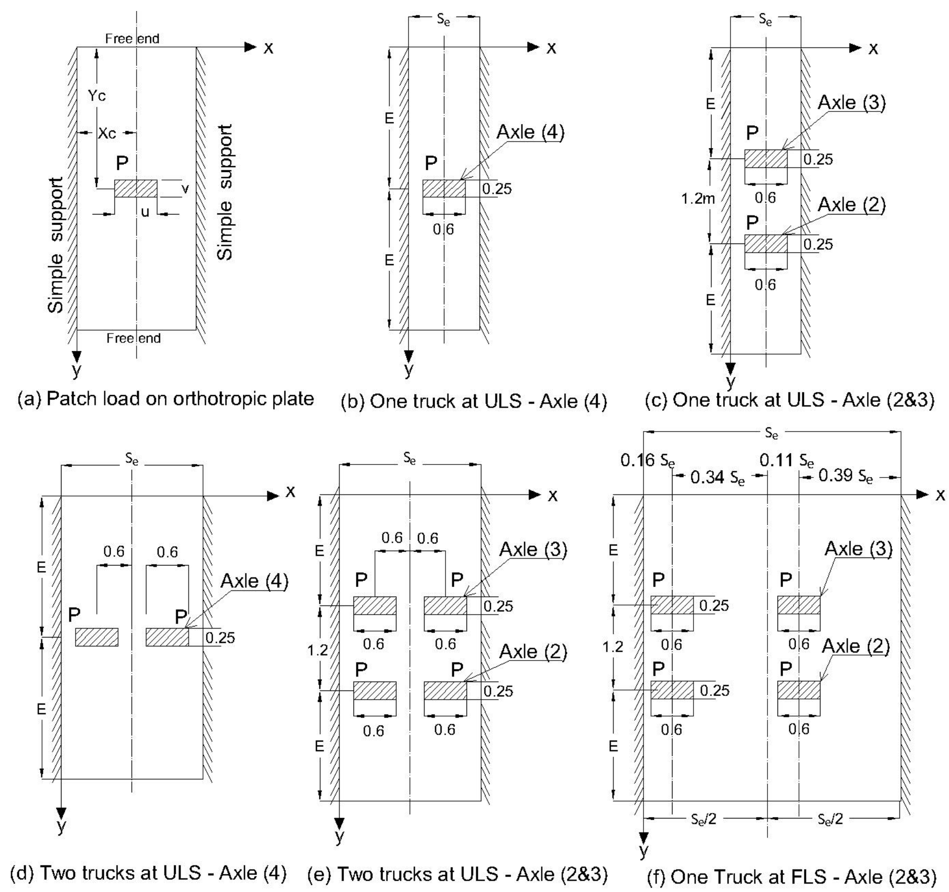

Fig. 3. Orthotropic plates subjected to uniformly loaded patch loads

The applied wheel load was calculated as P_{wheel} (1+DLA) R_L. P_{wheel} was taken as the wheel load shown in Fig. 2. The dynamic load allowance (DLA) was taken as 0.4 for the case of single axle, 0.3 for the case of axles 2 &3, and 0.25 for the case of 5 axles [1]. The modification factor for multilane loading, R_L, was 1 for a single truck case and 0.9 for a two-adjacent truck case [2].

The deck slab under consideration has a span, being the spacing between longitudinal girders, and width equals the girder length. PLATO program models plates of span and width shown in Fig. 3(a). Higgins [13] showed that the deflections and moments diminish as the transverse distance from the load application increases, and when the distance from the load point is more than twice the span length, these are negligible. So, in this research, the overall plate width, B, used for the orthotropic plate analyses for the loading case in Fig. 3(b) was taken four times the span length (i.e., B= 2E = 4 S_e). For the loading case in Fig. 3(c), the overall plate width used for the analyses was taken four times the span length in addition to the distance between axles 2 and 3 (i.e., B = 2E + 1.2 m = 4 S_e).

4. Results and Discussions

The results from the parametric study were presented in the form of a transverse moment in the normal girder direction, $M_{trans.}$, a longitudinal moment in the direction of traffic, $M_{long.}$, and deflection, Δ_L. Six loading scenarios (LS) were considered in this study at ULS. LS1 represented axle 4 for the single truck, as depicted in Fig. 3(b), and LS2 represented axle 4 in the case of two adjacent trucks, as depicted in Fig. 3(d). LS3 represented axles 2 & 3 for single truck as depicted in Fig. 3(c), LS4 represented axles 2 & 3 in case of two adjacent trucks as depicted in Fig. 3(e). LS5 and LS6 are identical to LS3 and LS4 except all truck axles are considered. Figure 4 shows sample results for the transverse moments obtained from each load scenario for D of 1 and different slab spans. One may observe that the load scenario with axle 4 in a single truck case (LS1) produced the greatest transverse moment for slab spans up to about 2.8 m, beyond which LS4 with axles 2 &3 for twin truck case provided the greatest moment among other load scenarios.

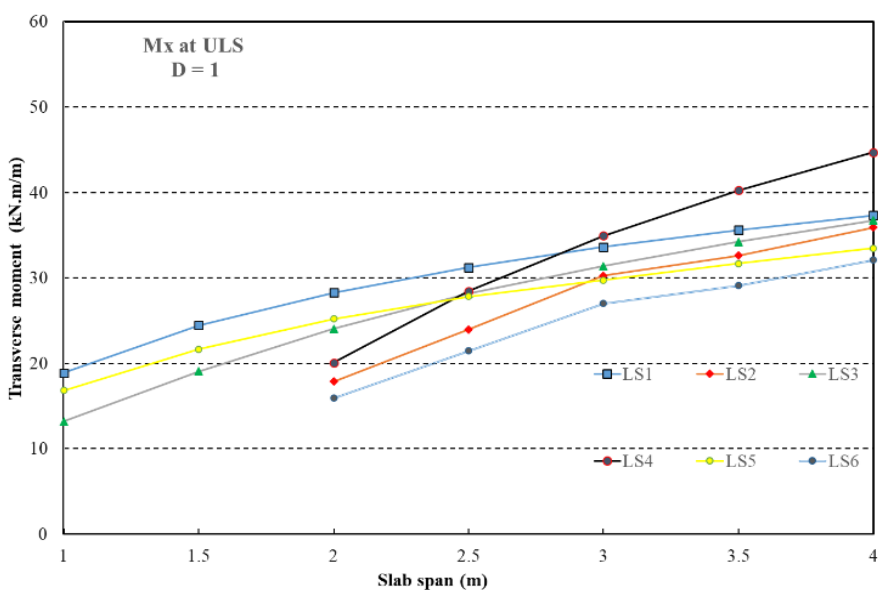

Fig. 4. ULS transverse moment in RC slab with difference load scenarios.

4.1. Transverse Moment

Figure 5 compares the ULS transverse moment from different stiffness ratios, D, and the moment from equation 2 specified in CSA-S6-19. One may observe that the transverse moment increases with the increase in slab stiffness ratio. Also, the transverse moment increases with the increase in slab span, as expected. The results show that the code equation does not have a trend concerning the change of D values. This indicates the need to change this equation to include the flexural stiffness ratio as a parameter.

For fatigue limit state (FLS) load scenarios, considering axles 2 & 3, Fig. 5 shows the change in the transverse with the change in flexural stiffness ratio and slab span. One may observe that the transverse moment increases with the increase in D values. As for the comparison with the code equation, it can be observed that equation (1) provides transverse moment greater than those obtained for all D values considered in this study. This is expected since equation (1) considered axle 4 of the truck which is much heavier than axle 2 or 3. This shows the necessity to develop moment equation for FLS design in addition to that for ULS design.

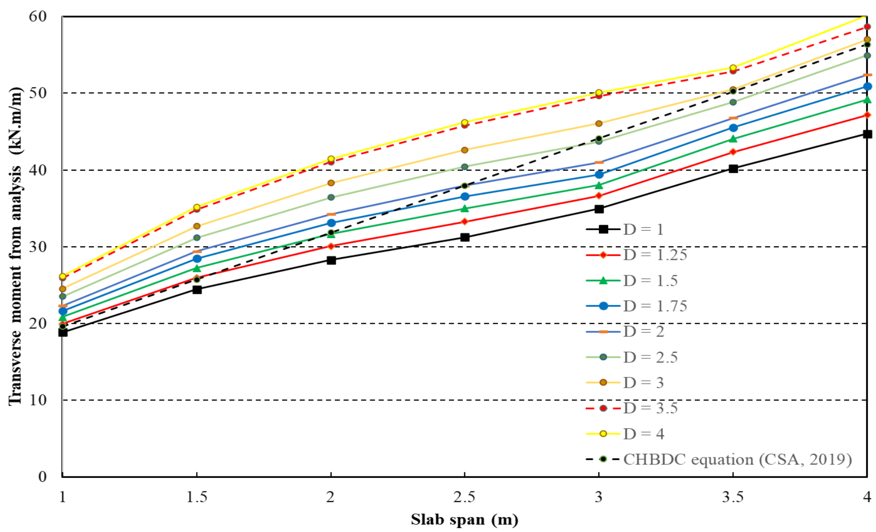

Fig. 5. ULS Transverse moment in RC slab with difference D ratios.

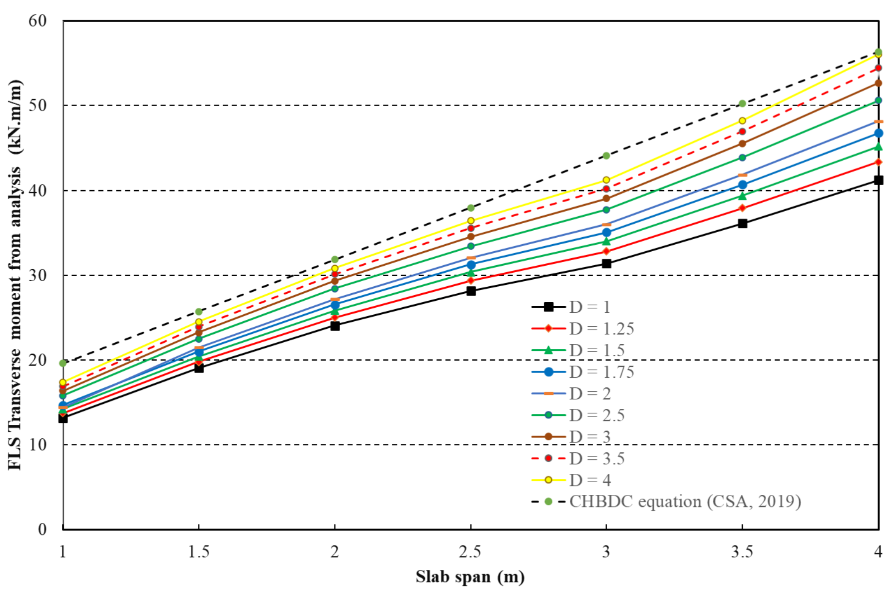

Fig. 5. FLS Transverse moment in RC slab with difference D ratios.

4.2. Longitudinal Moment

Figure 6 compares the ULS longitudinal moment from different stiffness ratios, D, and the moment based on the criteria mentioned in CSA-S6-19. One may observe that the longitudinal moment increases with the increase in slab stiffness ratio, and slab span as expected. The results show that the longitudinal moment values obtained from the code match those obtained from analysis for D of 1, while it is greater than those obtained with D values greater than 1 with a significant margin. For fatigue limit state (FLS) load scenarios, considering axles 2 & 3, Fig. 7 shows the change in the longitudinal moment with the change in flexural stiffness ratio and slab span. One may observe that the longitudinal moments obtained from the code provision are significantly greater than those obtained from the analysis irrespective of the flexural stiffness and span values.

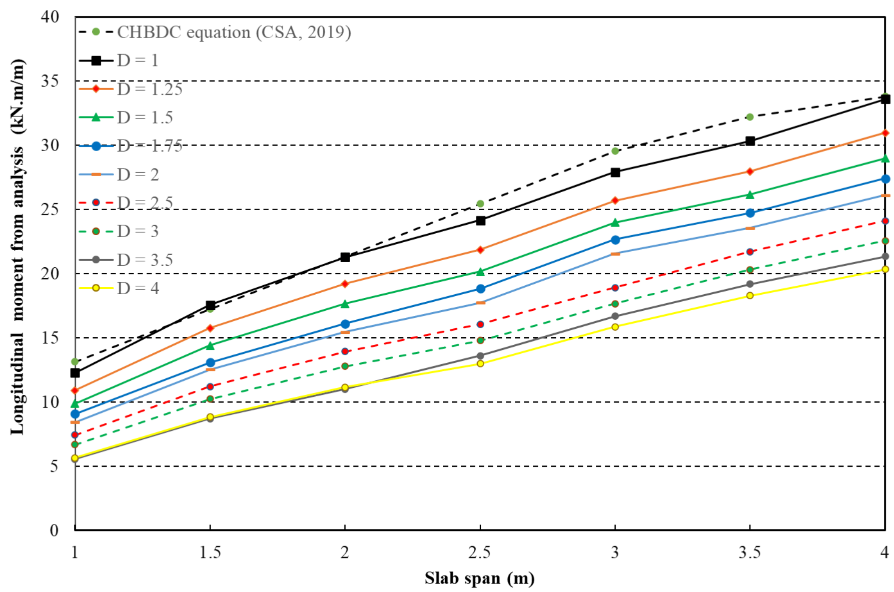

Fig. 6. ULS Longitudinal moment in RC slab with difference D ratios.

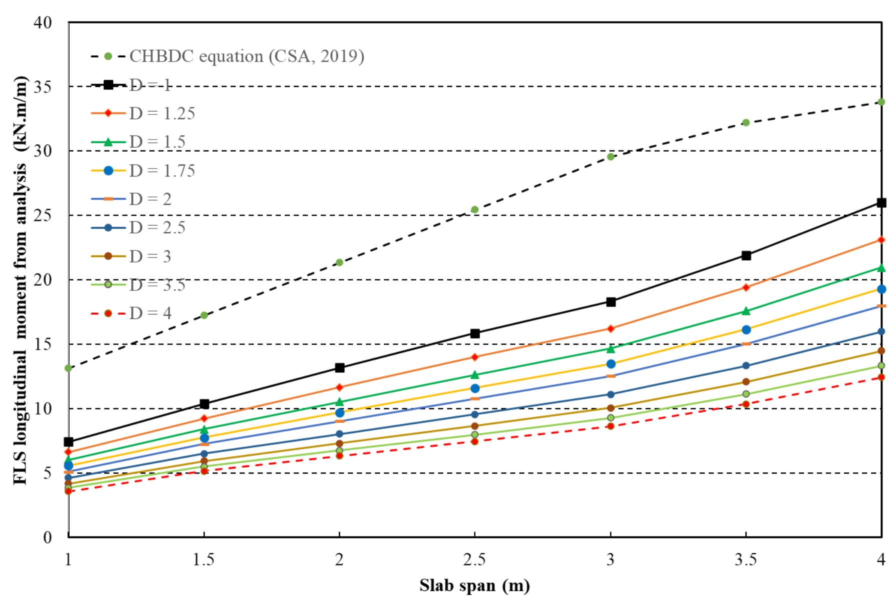

Fig. 7. FLS Longitudinal moment in RC slab with difference D ratios.

4.3. Slab Deflection

Figure 8 illustrates the maximum deflection from the load scenarios in the bridge slab of different flexural stiffness and span lengths. One may observe that the deflection increases with increase in slab span and stiffness ratio, however, rate of increase is much greater with the increase in span length than the stiffness ratio.

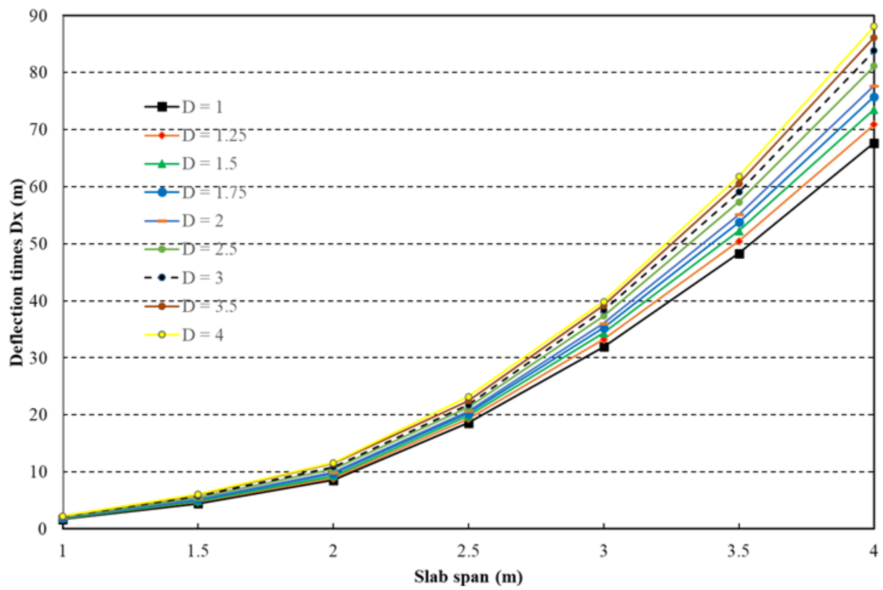

Fig. 8. Deflection in RC slab with difference D ratios.

4.4. Development of Equations for Transverse and Longitudinal Moments and Deflection for CL-625 truck

The data generated from the parametric study was used to develop empirical equations for the transverse and longitudinal moments for ULS and ULS, as well as the deflection at SLS2. The nonlinear curve fitting employed in Microsoft Excel software was used to develop the equations in Table 1. These equations were developed while ensuring that the maximum underestimation of the design values is less than 5% [1].

Table 1: Maximum moments and deflections due to unfactored CL-625 truck wheel loads (including dynamic load allowance)

Condition	Design parameter	Span limit	Flexural rigidity ratio, D
ULS	$M_{trans.} = 19.1\ C\ S_e^{0.58} D^{0.25}$	$1\ m \leq S_e \leq 4\ m$	$1 \leq D \leq 4$
	$M_{long.} = 12.2\ C\ S_e^{\ 0.84}\ D^{(-0.5)}$	$1\ m \leq S_e \leq 2\ m$	
	$M_{long.} = 11.5\ C\ S_e^{\ 0.78}\ D^{(-0.39)}$	$2\ m \leq S_e \leq 4\ m$	
FLS	$M_{trans.} = 13.5\ C\ S_e^{\ 0.8}\ D^{0.2}$	$1\ m \leq S_e \leq 4\ m$	
	$M_{long.} = (1.87 + 5.6\ S_e)\ D^{(-0.52)}$	$1\ m \leq S_e \leq 2\ m$	
	$M_{long.} = (-2.06 + 6.94\ S_e)\ D^{(-0.54)}$	$2\ m \leq S_e \leq 4\ m$	
SLS2	$\Delta_L = (1800\ C\ S_e^{\ 2.3}\ D^{0.2})\ /\ D_x$	$1\ m \leq S_e \leq 2\ m$	
	$\Delta_L = (1800\ C\ S_e^{\ 2.65}\ D^{0.2})\ /\ D_x$	$2\ m < S_e \leq 4\ m$	

Notes: C = continuity factor, taken as 1 for simple span deck slabs and 0.8 for the deck slabs continuous over three or more supports; S_e = deck slab span between girders; D = Transverse-to-longitudinal stiffness ration (D_x/D_y); ULS =: ultimate limit state; FLS = fatigue limit state; SLS2 = second combination of serviceability limit state [1].

3. Conclusions

The current CHBDC code provisions provide a method for calculating the design moment in concrete slab bridge deck, deck, which may not provide conservative estimates of the maximum live load moment as it does include the effect of the the flexural stiffness ratio. A parametric study was conducted on a simply-supported slab using the orthotropic plate theory theory to determine the applied transverse and longitudinal moment and deflection under different truck loading conditions, conditions, flexural stiffness ratio, and span lengths. Results showed the drawback of the code equation. Also, results show that the transverse moment and deflection increase with the increase in flexural stiffness ratio while the longitudinal deflection decreases. The data generated from this study was used to develop empirical equations for the transverse and longitudinal moments for ultimate and fatigue limit state design and deflection for serviceability limit state design.

References

[1] CSA. (2019). Canadian Highway Bridge Design Code, CSA-S6:19, Canadian Standard Association, Toronto, Ontario, Canada.

[2] Westergaard, H. M. (1930). Computation of Stresses in Bridge Slabs Due to Wheel Loads. United States Govt. Printing Office.

[3] CSA. (1988). Design of Highway Bridges, CSA-S6:88. Canadian Standard Association, Toronto, Ontario, Canada.

[4] AASHTO. (1996). Standard Specifications for Highway Bridges. American Association of State Highway Officials, Washington, D.C.

[5] AASHTO. (1998). AASHTO LFRD Bridge Design Specifications. American Association of State Highway Officials, Washington, D.C.

[6] AASHTO. (2020). AASHTO LFRD Bridge Design Specifications. American Association of State Highway Officials, Washington, D.C.

[7] Cusens, A. R., & Pama, R. P. (1975). Bridge Deck Analysis. London, England: John Wiley and Sons Inc.

[8] Timoshenko, S. P., & Woinowsky-Kreiger, S. (1959). Theory of Plates and Shells. Mc-Graw Hill.

[9] Troistky, M.S. (1968). Orthotropic Bridges – Theory and Design. The James F. Linoln Arc Welding Foundation, USA.

[10] Bakht, B., Mufti, A. A., & Desai, Y. M. (2003). PLATO User Manual: Analysis of Orthotropic Plates. ISIS Canada Research Network.

[11] Chatha, N. (2022). Load Distribution in Shear-Connected Adjacent Precast Girder Bridges under CHBDC Truck Loading. M.A.Sc. Thesis, Toronto Metropolitan University, Toronto, Canada.

[12] Sennah, H. (2020). Structural Behaviour of Shear-Connected Adjacent Precast Concrete Box Beam Bridges Subjected to AASHTO Truck Loading. M.A.SC. Thesis, Toronto Metropolitan University, Toronto, Canada.

[13] Higgins, C. (2003). LRFD Orthotropic Plate Model for Live Load Moment. Journal of Bridge Engineering, 8(1), 20-28.